Analytical and Bioanalytical Chemistry
https://doi.org/10.1007/s00216-021-03396-3

PAPER IN FOREFRONT

Ultra-high-performance liquid chromatography charge transfer dissociation mass spectrometry (UHPLC-CTD-MS) as a tool for analyzing the structural heterogeneity in carrageenan oligosaccharides

Praneeth M. Mendis[1] · Zachary J. Sasiene[1] · David Ropartz[2,3] · Hélène Rogniaux[2,3] · Glen P. Jackson[1,4]

Received: 8 February 2021 / Revised: 16 April 2021 / Accepted: 7 May 2021

Abstract
Ultra-high-performance liquid chromatography (UHPLC) with charge transfer dissociation mass spectrometry (CTD-MS) is presented for the analysis of a mixture of complex sulfated oligosaccharides. The mixture contained kappa (κ), iota (ι), and lambda (λ) carrageenans that contain anhydro bridges, different degrees of sulfation ranging from one to three per dimer, different positioning of the sulfate groups along the backbone, and varying degrees of polymerization (DP) between 4 and 12. Optimization studies using standard mixtures of carrageenans helped establish the optimal conditions for online UHPLC-CTD-MS/MS analysis. Optimization included (1) UHPLC conditions; (2) ion source conditions, such as the capillary voltage, drying gas and nebulizing gas temperature, and flow rate; and (3) CTD-MS conditions, including data-dependent CTD-MS. The UHPLC-CTD results were contrasted with UHPLC-CID results of the same mixture on the same instrument. Whereas CID tends to produce B/Y and C/Z ions with many neutral losses, CTD produced more abundant A/X ions and less abundant neutral losses, which enabled more confident structural detail. The results demonstrate that He-CTD is compatible with the timescale of UHPLC and provides more structural information about carrageenans compared to state-of-the-art methods like UHPLC-CID analysis.

Keywords Highly sulfated oligosaccharides · Ion-pair reagent · Radical ion fragmentation · High-energy activation · Charge transfer dissociation

Introduction

Carbohydrates are among the most abundant and structurally diverse biomaterials found on earth [1]. The inherited structural complexity of carbohydrates has evolved to perform diverse roles in nature. Biologically relevant carbohydrates have participated in crucial processes in living organisms, such as in cell-cell recognition, cell interactions, and maintaining the structural integrity of cells [2]. Among those biologically relevant carbohydrates, sulfated polysaccharides have attracted considerable attention due to the significant roles they play in living organisms. Carrageenans are a subclass of sulfated polysaccharides that are extracted from the cell wall of marine red seaweeds, *Rhodophyta* [2], and they provide both structural rigidity to the seaweeds and cell-cell recognition between host cells and pathogen cells [2, 3]. Nearly 90% of the world's carrageenans comes from *Kappaphycus* and *Eucheuma* seaweeds that are cultivated in Indonesia and the Philippines [4]. Carrageenans are widely used as thickening and gelling ingredients in the food and pharmaceutical industries [3, 5]. Carrageenan oligosaccharides are considered as potential therapeutic products with immunomodulatory [6], antihyperlipidemic [7], anticoagulant [8], anti-inflammatory, and antioxidant properties [9]. More importantly, in many

Published in the topical collection celebrating *ABCs 20th Anniversary*.

✉ Glen P. Jackson
glen.jackson@mail.wvu.edu

[1] C. Eugene Bennett Department of Chemistry, West Virginia University, Morgantown, WV 26506-6121, USA

[2] INRAE, UR BIA, 44316 Nantes, France

[3] INRAE, BIBS Facility, 44316 Nantes, France

[4] Department of Forensic and Investigative Science, West Virginia University, Morgantown, WV 26506-6121, USA

Published online: 29 May 2021

studies, highly sulfated carrageenans have shown antiviral activity against the hepatitis A virus (HAV) [10], herpes simplex virus (HSV) [11, 12], influenza A virus (IAV) [13, 14], and dengue virus [15, 16]. These biological and unique physiochemical properties of carrageenans correlate with the position and number of sulfate groups on the sugar residues along with the degree of polymerization (DP) of the structure [3, 9, 17]. Therefore, the detailed structural analysis of carrageenans not only assists in the identification of the chemical properties that lead to the significant physio-chemical behavior of these sugars but also provides information regarding the relationship between the structure and biological activity of these compounds.

Carrageenans have a primary structure that is polymeric in nature and consists of a linear chain of alternating 1,3-linked β-D-galactose (G) and 1,4-linked α-D-galactose (D) disaccharide repeating units [18]. They are classified into subclasses, according to the number and position of the substituents of the sulfate ester group and the presence of anhydrous bridges to make 3,6-anhydrogalactose (DA) units. Among these subclasses, the three mainly exploited in industry are kappa *(κ)*, iota *(ι)*, and lambda *(λ)* carrageenans. Their structures are presented in Fig. 1 [18, 19]. κ-Carrageenans are built of a DA monomer and a G monomer with C4 sulfation (G4S), which together represents a repeating polymer of the form $(DA\text{-}G4S)_n$. ι-Carrageenans are built of a DA monomer with C2 sulfation (DA2S) and a G monomer with a sulfate group at C4 (G4S) position, which is depicted as $(DA2S\text{-}G4S)_n$. λ-Carrageenans are highly sulfated and the repeating unit contains a D monomer with C2 and C6 sulfation (D2S,6S) and a G monomer with a sulfate group at C2 (G2S), which is shown as $(D2S,6S\text{-}G2S)_n$. Carrageenans differ from GAGs mainly by their unique monosaccharide composition. GAGs contain *N*-acetylglucosamine, *N*-acetylgalactosamine, glucuronic acid, and iduronic acid units with 2-*O*/*N*, 4-*O*, and 6-*O* linked sulfation patterns, whereas carrageenans have galactose units with 4-*O* and 6-*O* linked sulfation [17, 20, 21].

The structural heterogeneity among the subclasses of carrageenans can be attributed to the algal species, life stage, environmental conditions, and the extraction procedure of the polysaccharide [2, 18, 22]. κ-Carrageenan and ι-carrageenan are produced from *Kappaphycus* and *Eucheuma* species, respectively. λ-Carrageenans are produced from cold-water species such as *Gigartina skottsbergii*, *Chondrus crispus*, and *Mastocarpus stellatus* [4, 23]. The cold-water species produce another important carrageenan type called hybrid carrageenans, which consist of *kappa-iota* hybrids, *kappa-lambda* hybrids, and *kappa*-2-hybrids [4]. Hybrid carrageenans lead to the production of heterogenous grade carrageenan with different rheological properties [4]. Enzymes such as κ-, ι-, and λ-carrageenases are used to produce oligosaccharides from polysaccharides carrageenans by cleavage of the internal β-(1-4) linkages of κ-, ι-, and λ-carrageenans [24]. Due to the complex nature and lability of the sulfate substituents, these compounds are difficult to analyze; therefore, effective analytical tools are needed to characterize these complex carrageenans.

Nuclear magnetic resonance (NMR) spectroscopy is a powerful tool applied in the characterization of carrageenan oligosaccharides [25, 26], but the time-consuming purification procedures and requirement of hundreds of micrograms or more of sample limit the use of NMR for structural analysis [18]. Unlike NMR, mass spectrometry techniques are generally compatible with separations and enable faster analyses of more complex mixtures and with significantly smaller sample sizes [27]. Tandem mass spectrometry (MS/MS) is particularly effective for the structural analysis of oligosaccharides [28, 29].

In tandem mass spectrometry, glycosidic cleavages such as B/Y and C/Z ions help provide the general saccharide composition, whereas cross-ring fragments such as A/X ions help identify the linkage and the branching patterns [28, 29]. Collision-induced dissociation (CID) is a widely used MS/MS technique for oligosaccharides [29, 30], even for sugars containing sulfate modifications, such as glycosaminoglycans (GAGs) [31]. However, CID is generally more likely to

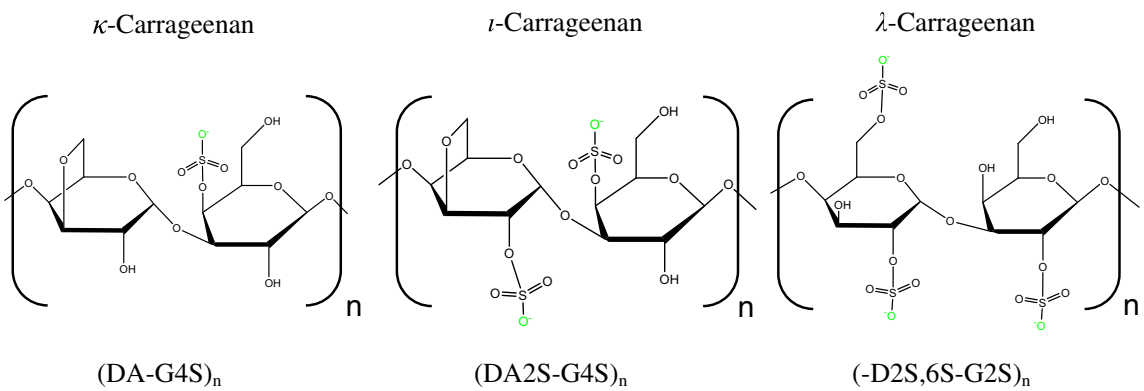

Fig. 1 Different repeating unit compositions of carrageenans

generate glycosidic fragments than the more structurally informative cross-ring fragments [21, 32, 33]. In addition, CID tends to produce abundant, uninformative neutral losses and consecutive fragments, especially of the labile sulfate modifications. Therefore, CID often fails to provide some of the most important detailed structural information [17, 33].

As alternatives to CID, electron- and ion-based MS/MS techniques have been used for the analysis of sulfated oligosaccharides, including glycosaminoglycans (GAGs) and carrageenans [21, 33–35]. Electron- and ion-based MS/MS techniques, such as electron capture dissociation (ECD) [36], electron-induced dissociation (EID) [37], electron detachment dissociation (EDD) [34], and negative electron transfer dissociation (NETD) [35] have all been successfully applied to sulfated oligosaccharides. ECD of κ-carrageenans provided informative fragments in the presence of divalent metal adducts [36], but ECD can only be applied to multiply charged positive ions, which limits the applicability towards highly acidic and neutral oligosaccharides [36]. In EDD, multiply charged anions undergo radical-driven fragmentation processes after irradiation with approximately 19 eV electrons [33]. EDD can produce sulfate-retaining glycosidic and cross-ring cleavage products, which helps to determine the site of sulfation [34, 38].

NETD is another fragmentation technique in which gas-phase electron transfer occurs at thermal energies between the analyte anion to a rare gas cation [35, 39]. Both EDD and NETD are capable of providing sufficient fragmentation to distinguish epimers of GAGs [40]. In the analysis of complex mixtures, the activation times of NETD are amenable to chromatographic coupling, but EDD requires longer activation times and is not as compatible to chromatographic coupling [40]. EDD and NETD are typically applied to precursor ions with a charge state ≥2 [34, 35], whereas EID can be used for singly and multiply charged negative ions [37]. Even though ECD, EDD, and EID often produce more structural information compared to CID, they tend to be restricted to Fourier-transform ion cyclotron resonance (FTICR) mass analyzers, which are cost-prohibitive for most laboratories. ECD and EID have recently been implemented on benchtop, hybrid instruments, but the figures of merit are still under assessment [41].

Photon-based MS/MS techniques can also provide useful fragments including cross-ring cleavages with sulfated oligosaccharides [40, 42]. Ultraviolet photodissociation (UVPD) and extreme ultraviolet dissociative photo-ionization (XUV-DPI) are widely used photon-based MS/MS techniques that have shown promising results for GAGs, carrageenans, and porphyrans [40, 43]. UVPD produces sulfate-retaining glycosidic and cross-ring fragments in shorter times compared to EDD, which is a useful feature for online analysis of complex mixtures [40]. Softer wavelength UVPD requires a chromophore derivative to be bound to the native oligosaccharides and potentially limit the structural information [42, 44], but vacuum-UV (VUV-PD) does not require specific chromophores [45–48]. XUV-DPI has been shown to provide efficient fragmentation by using photons in excess of 18 eV from a synchrotron radiation source [43]. However, XUV-DPI has been restricted to the use of specialized laboratories due to the limited access to synchrotron radiation sources.

Free-radical-activated glycan sequencing (FRAGS) reagent is an alternative method based on free-radical-driven dissociation techniques [49]. The FRAGS reagent can selectively conjugate to the reducing terminus of the glycan and, upon collisional activation, the FRAGS reagent generates a free-radical, which simultaneously induces both glycosidic and cross-ring fragmentation without glycan rearrangements and internal or external residue losses [49, 50].

Helium charge transfer dissociation (He-CTD) uses a kiloelectronvolt beam of helium cations to ionize and fragment precursor ions [51], and it has provided promising results for oligosaccharides [32, 52], peptides [51], proteins [53], and lipids [54]. Prior to the development of He-CTD, Schlathölter's group and Zubarev's group performed valuable experiments involving cation-cation reactions at elevated kinetic energies [55–57]. Schlathölter's group showed that helium cations in the region of 2–10 keV have the ability to abstract an electron from a singly charged protonated precursor ion and form a doubly charged radical ion via two different pathways: electron stopping and charge transfer [55, 57]. In both mechanisms, excess energy allows radical-driven fragmentation of the target ions [32, 51, 54], but electron stopping is dominant and provides significantly higher excitation energies than charge transfer. Hoffman and Jackson used the distribution of product ions following the He-CTD fragmentation of neutral chloroform in the trap to estimate that the average energy during activation is in the range of 30–40 eV [51], which is significantly higher than the excitation energy available through pure charge transfer.

He-CTD has been successfully applied to the characterization of sulfated oligosaccharides, including GAGs and carrageenans [17, 21, 32, 58]. He-CTD provided structurally informative fragments that were similar to EDD and XUV-DPI and included glycosidic and cross-ring fragments from highly acidic sulfated compounds. He-CTD preserved the sulfate groups on many fragments and therefore enabled the localization of labile sulfate ester modifications [17, 21]. In addition, He-CTD has been used to distinguish the β-1,4- and β-1,3-linked native oligosaccharides, which is a useful tool for in-depth structural analysis in carbohydrate research [58].

Before analysis, enzymatic degradation using carrageenases is typically performed to produce lower molecular weight oligosaccharides. Such enzymolysis typically leads to a more complex carrageenan mixture [2, 9]. Strong anion exchange chromatography (SAX) would be the ideal method to separate the highly ionized sulfated oligosaccharides [59, 60], but SAX separations achieved under high alkaline and/or salt concentration are not

compatible with online MS analysis [59, 61]. Size exclusion chromatography (SEC) has been used to separate depolymerized GAGs of different lengths [62, 63], but the resolution of SEC is generally not as good as other LC techniques [20, 59]. Hydrophilic interaction liquid chromatography (HILIC) has been widely used for separation of sulfated oligosaccharides [64], and the elution order correlates with the polarity of oligosaccharides, which is readily determined by the size, sulfation, and acetylation content [59, 64]. Successful implementation of HILIC LC-NETD-MS/MS for structural characterization of heterogenous sulfated oligosaccharides has been reported in recent studies [65]. Although HILIC separation is sensitive to the oligosaccharide chemical composition and compatible with online ESI-MS, HILIC does not separate isomers effectively [64]. Porous graphitic carbon (PGC) chromatography uses hydrophobic and electronic interactions between the analyte and the stationary phase and has been used to separate *κ- and ι*-carrageenan oligomers [18, 26]. However, many groups report that long conditioning times are required between runs to provide reproducible retention times [66].

Ion-pair reversed-phase HPLC (IP-RP-HPLC) is a promising technique that uses alkyl ammonium salts and a reversed phased resin to separate charged analytes [20, 67]. IP-RP-HPLC has been used to separate carrageenans, GAGs, and heparin isomers, and the order of elution is related primarily to the number of free sulfate modifications and secondarily to the oligomer length [2, 59, 61, 68, 69]. Some of the advantages of online analysis with IP-RP-HPLC are (1) requirement of lower salt concentrations, which is compatible with mass spectrometric detection; (2) removal of alkaline earth metal cations from the oligosaccharide sample mixture; and (3) stabilization of the sulfate groups and preventing their decomposition in the ESI source [2, 68].

The work herein demonstrates that CTD-MS/MS can operate on a timescale compatible with IP-RP-UHPLC for the analysis of a complex carrageenan mixture derived from red algae *Rhodophyta*. The obtained results from IP-RP-UHPLC-CTD-MS/MS were compared with IP-RP-UHPLC-CID-MS/MS to evaluate the relative effectiveness of the two techniques. The described IP-RP-UHPLC-CTD-MS/MS method led to the structural characterization and differentiation of carrageenan oligomers of different lengths, structures, and extents of sulfation, and shows promise for future applications involving complex mixtures of anionic oligosaccharides.

Experimental

Reagents and oligosaccharides

Hexylamine (HA) was purchased from Sigma-Aldrich. Formic acid (FA), HPLC-grade methanol (MeOH), and Optima® LC/MS grade Acetonitrile (ACN) were purchased from Fisher Scientific (Fair Lawn, NJ). Ultra-pure 18 MΩ water was obtained from a Milli-Q apparatus from Millipore. Oligosaccharides were produced by the laboratory CNRS-UPMC UMR 8227, Station Biologique, (Roscoff, France). κ-Carrageenans from *Euchema Cottonii* (Cottoni X-6913, CPKelco), ι-carrageenan from *Eucheuma denticulatum* (ref 2544-88-02, Danisco), and λ-carrageenan from *Gigartina skottsbergii* (ref 2544-89-01, Danisco) were degraded enzymatically into oligosaccharides using κ-carrageenase, ι-carrageenase, and λ-carrageenase, respectively. For all samples, purification was carried out by size exclusion chromatography. The complex mixture of carrageenans was prepared using individual carrageenan samples.

Ion-paired reversed phase chromatography separation

Chromatographic separation was performed on a Shimadzu Nexera X2 UHPLC system (Kyoto, Japan) using a Waters BEH C18 column with the following dimensions: 100 mm × 1.0 mm, packed with 1.7 μm particles (Wexford, Ireland). The flow rate was set to 0.15 ml/min and the column heater was set to 40 °C. A binary gradient was used for separation with mobile phase A consisting of pure water with 25% of 20 mM hexylamine and mobile phase B consisting of pure ACN with 25% of 20 mM hexylamine. The pH of the 20 mM hexylamine was adjusted to pH 6 by the addition of acetic acid. The gradient was increased linearly from 16.6 to 35% of solvent B for 10 min, then raised linearly from 35 to 63.4% between 10 and 20 min, then increased linearly from 63.4 to 73.4% between 20 and 24.50 min. Re-equilibration of the column was performed between 24.51 and 32.50 min with 16.6% of solvent B to resemble initial elution conditions.

He-CTD

He-CTD was performed on a modified amaZon ETD quadrupole ion trap from Bruker Daltonics (Bremen, Germany), the details of which are described elsewhere [51, 70]. Briefly, a saddle field fast ion source from VSW/Atomtech, (Macclesfield, UK) was fixed above a 2-mm hole in the ring electrode of the 3D ion trap and connected to a variable leak valve (Model 203, Granville-Phillips) to control the flow of helium gas through the fast ion source, which typically raised the pressure of the main vacuum chamber by ~1×10^{-5} mbar. The ion source was connected to an economical home-built system that employs an Ultravolt HVA series high voltage power supply (Advanced Energy, Denver, CO, USA). The +7.5 kV high voltage from the Ultravolt UHA was pulsed from ground to high voltage with rise times as fast as 5 ns by using a Behlke 101-03 switch (Behlke, Billerica, MA, USA). A TTL signal was taken from the MS^2 event of the Bruker amaZon and sent to an Agilent 33250A arbitrary

function generator (AFG) (Keysight Technologies, Santa Rosa, CA, USA), to provide an independently variable delay and pulse width. A DS1054 digital oscilloscope (Rigol, Beaverton, OR, USA) compared the trigger waveform from the AFG with the scan function of the Bruker amaZon to ensure that the high voltage pulses coincided with the desired storage period of the scan function. The saddle field fast ion source has an 85% conversion efficiency. Therefore, the +7.5 kV anode voltage generates helium cations with a maximum kinetic energy of approximately 6.6 keV and a mean energy closer to 6.4 keV. The saddle field fast ion source pulse was matched with the fragmentation portion of the scan function of the instrument with the CID amplitude set to 0.

Online CTD-MS

The effluent from the UHPLC was connected to the standard Apollo electrospray ionization source (Bruker Daltonics, Billerica, MA). The capillary voltage and end cap voltage were set to −4500 V and − 500 V, respectively. The nebulizer pressure was set to 30 psi, and the dry gas flow rate and dry gas temperature were set to 4 L/min and 150 °C, respectively. Experiments were conducted in data-dependent acquisition (DDA) mode from *m/z* 150–2000. The most abundant charge state of each analyte was chosen as the precursor ion. The precursor ions were isolated with a window of 8 Da to prevent unwanted fragmentation of the fragile sulfate groups, and the CID collision energy was set at 0 (arbitrary units) to prevent CID when CTD was active. The fast ion gun was pulsed on for 50 ms and the product ions were stored for an additional 150 ms after activation to help reduce the observed chemical background. As a comparison to CTD, data of the same carrageenan mixture using the same UHPLC conditions was also collected using traditional CID on the same instrument with a CID collision energy at 0.70 V and a 200 ms activation time. For online UHPLC-CID, smart fragmentation was turned on and set to ramp from 80 to 120% of the CID collision energy. The low mass cutoff was set to 27% of the precursor ion.

Data analysis

Raw data were transformed in Bruker Compass Data Analysis 4.0 SP4 software and further processed using Microsoft Excel (Microsoft, Redmond, WA, USA). The peaks in the deconvoluted spectra were chosen manually based on their signal-to-noise ratio, isotope envelope distribution, and fragmentation patterns. Peaks also had to appear in at least five replicate spectra across chromatographic peaks to be considered sufficiently reliable for identifications. Product ion assignments for LE-CID (low-energy CID) and He-CTD were achieved using an in-house analysis database made in Excel. Product ion mass accuracies were typically better than 0.05 Da and no larger than 0.25 Da. ChemDraw 19.1 (PerkinElmer, Walthman, MA, USA) was used for chemical structure illustrations.

Results and discussion

The focus of this study is to resolve the structures of sulfated oligosaccharides, namely carrageenans extracted from the cell wall of marine red seaweeds *Rhodophyta*. These carrageenans are present with repeating sulfation patterns and are good sources of oligosaccharides with specific sulfation positioning [71]. The complex mixture contained various carrageenans, including κ, ι, and λ structures with varying degree of polymerization, sulfation, and different positioning of the sulfate groups along the backbone. The carrageenan mixture was separated using IP-RP-UHPLC prior to MS analysis. Figure 2 shows the total ion chromatogram (a) and the reconstructed total ion chromatogram (b) of the complex mixture. The elution order of the carrageenan components is governed primarily by the number of sulfate groups interacting with IP agents, thus by the type of carrageenan [20, 43]. The retention times are affected secondarily by the DP of each carrageenan category, where longer DP structures have longer retention times [2, 59]. κ-DP4 has two sulfate groups and elutes first at 1.4 min using the conditions provided in the experimental section. Following κ-DP4 is κ-DP6 with three sulfate groups (at 2.6 min), κ-DP8 with four sulfate groups (at 3.7 min), and κ-DP12 with six sulfate groups (at 5.4 min). Others have shown that IP-RP chromatography is able to separate κ-carrageenans up to $(DA\text{-}G4S)_{16}$ while preserving the integrity of the molecules [2]. ι-DP6 contains a total of six sulfate groups present for three dimeric units and elutes at 5.9 min. Finally, λ-DP6 and λ-DP8 with three sulfate units per dimer unit eluted last. Sulfated oligosaccharides yielded precursor ions in either the 1+ or 2+ charge state, which were formed by having one or two more IP reagents, respectively, than the number of sulfate groups [2].

In addition to the efficient separation of the carrageenan mixture, IP-RP-UHPLC demonstrates the capability of maintaining the structural integrity of the eluting sulfated oligosaccharides by preserving the labile sulfate groups [2, 59]. Table 1 provides the separated carrageenans, their elution times, and the precursor ion *m/z* values that were isolated and exposed to LE-CID or He-CTD for structural characterization. All product ions observed are annotated based on the Domon and Costello nomenclature system [72]. Supplementary Information (ESM) Tables S1–S12 contain lists of identified fragment ions from LE-CID and He-CTD for each analyte.

Fig. 3 shows the LE-CID and He-CTD spectra obtained for the κ-carrageenan DP4 eluting at 1.4 min. The precursor ion in each spectrum is the $[M + 3IPRH]^+$ at *m/z* 1094.5. In Fig. 3a the LE-CID spectrum shows that the majority of the fragments

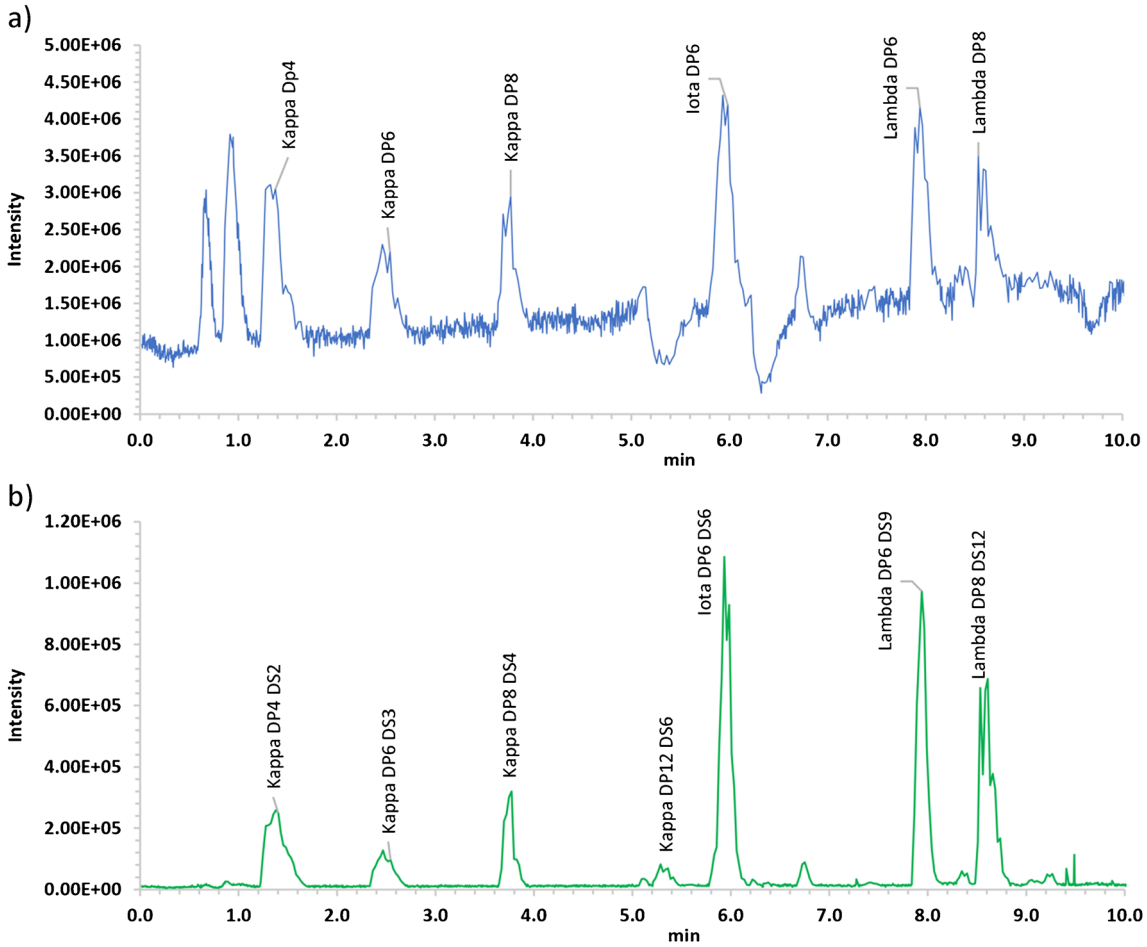

Fig. 2 Chromatograms of IP-RP-UHPLC separation of a complex mixture of enzymatically derived carrageenans: **a)** total ion chromatogram; **b)** reconstructed ion chromatogram of molecular ions obtained concurrently with Fig. 2**a**. (DP = degree of polymerization; DS = degree of sulfation)

are glycosidic bond cleavages [21, 27, 71]. Many fragments also contain neutral losses of IP reagent, SO_3, and H_2O, such as Y_3-IPR at *m/z* 849.32, Y_3-IPR-SO_3 at *m/z* 769.35, Y_3-2IPR-SO_3 at *m/z* 668.26, and Y_3-2IPR-2SO_3 at *m/z* 588.29. Single or multiple SO_3 losses are commonly seen with CID because they are facile low-energy rearrangement reactions [27, 36]. Glycosidic fragments are useful in identifying the general saccharide composition of the precursor, but the absence of cross-ring cleavages and the extensive neutral losses adds ambiguity to the saccharide composition and sulfate group localization [21].

In contrast to the LE-CID spectrum in Fig. 3a, the He-CTD spectrum in Fig. 3b shows a variety of cross-ring fragments and glycosidic cleavages throughout the structure, with an overall greater number of fragment ions compared to the LE-CID spectrum [17, 21, 32]. A systematic series of

Table 1 Summary of sulfated oligosaccharides separated using the IP-RP-UHPLC gradient that were exposed to either He-CTD or LE-CID. (DA = anhydro-D-galactose, G = β-D-galactose, D = α-D-galactose and numbers before an S indicates the location of any sulfate groups)

Oligosaccharide	MW (Da)	Nominal precursor *m/z* $[M+nIPRH]^{(n-\#s)+}$	Retention time (min)	# of sulfate groups (s)	Structure
κ-DP4	788.1	1094 (*n* =3)	1.4	2	$(DA\text{-}G4S)_2$
κ-DP6	1173.1	1582 (*n* =4)	2.6	3	$(DA\text{-}G4S)_3$
κ-DP8	1558.2	1085 (*n* =6)	3.7	4	$(DA\text{-}G4S)_4$
κ-DP12	2329.9	1573 (*n* =8)	5.4	6	$(DA\text{-}G4S)_6$
ι-DP6	1410.0	1114 (n=8)	5.9	6	$(DA2S\text{-}G4S)_3$
λ-DP6	1770.9	1413 (*n* =11)	7.9	9	$(D2S,6S\text{-}G2S)_3$
λ-DP8	2261.8	1265 (*n* =14)	8.5	12	$(D2S,6S\text{-}G2S)_4$

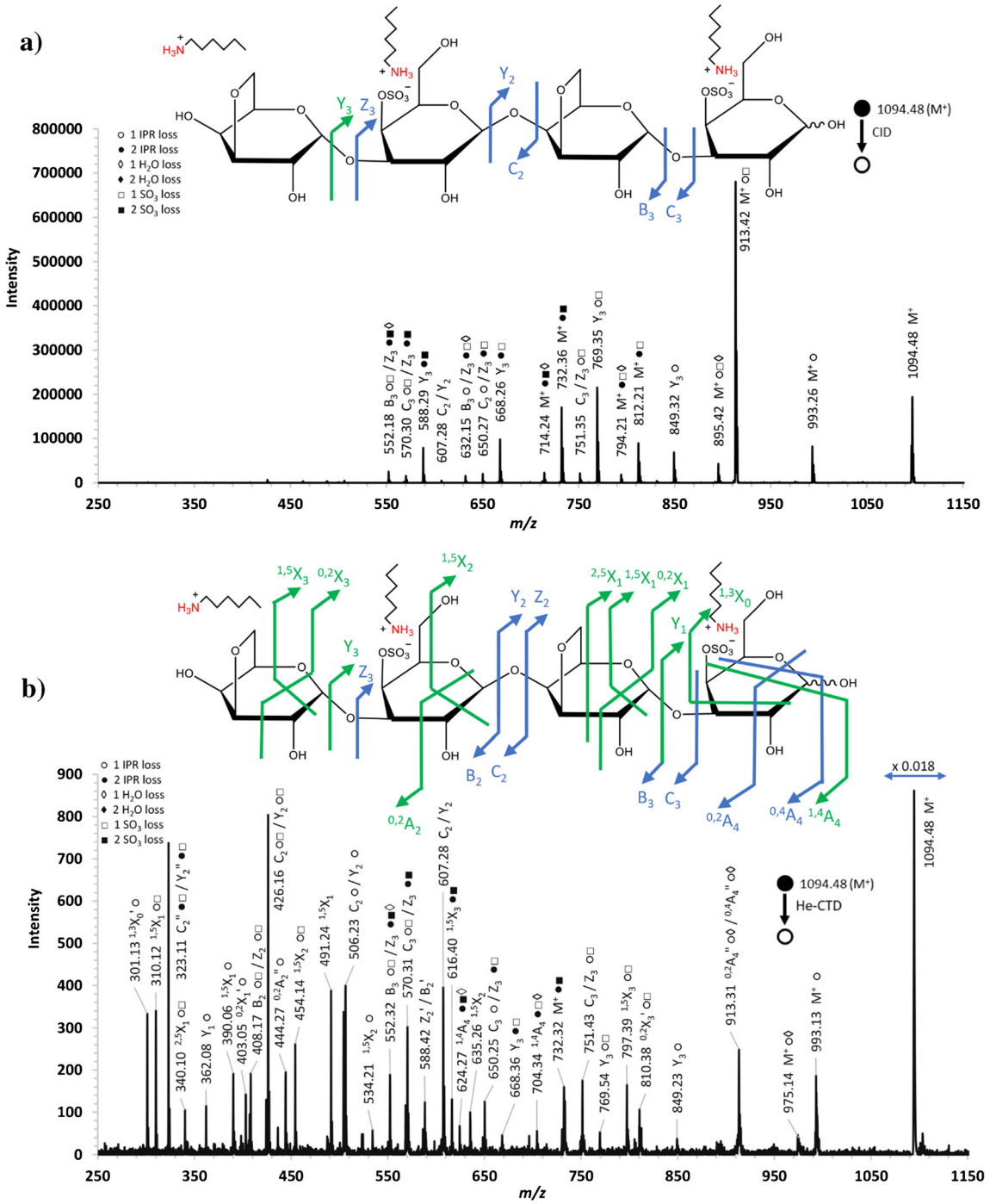

Fig. 3 IP-RP-UHPLC-MS/MS spectra of κ-carrageenan DP4 at 1.4 min collected in positive ion mode using **a)** LE-CID and **b)** He-CTD. The insets show the annotated product ions. Fragments with unambiguous assignments are annotated in green, whereas ambiguous assignments are annotated in blue. The notation M^+ in the labels refers to the precursor $[M + 3IPRH]^+$ species, which was selected as the isolated precursor ion at *m/z* 1094.48

structurally informative glycosidic fragments and cross-ring fragments, like $^{1,5}X_n$, $^{0,2}X_n$, and $^{0,2}A_n$ ions, are produced in the He-CTD spectrum of κ-DP4 [17]. Unlike CID, unambiguous localization of the sulfates on the backbone is possible with He-CTD because many of the fragments have retained the labile sulfate groups [17, 21]. These observations are similar to related work in which sulfate and IP groups retaining glycosidic and cross-ring fragments have been reported with XUV photo-dissociation (XUV-PD) for κ-DP6 in the presence of heptyl ammonium as the IP agent [43].

LE-CID and He-CTD spectra for κ-DP8 and κ-DP12 are shown in Fig. 4 and ESM Fig. S1, respectively. For κ-DP8,

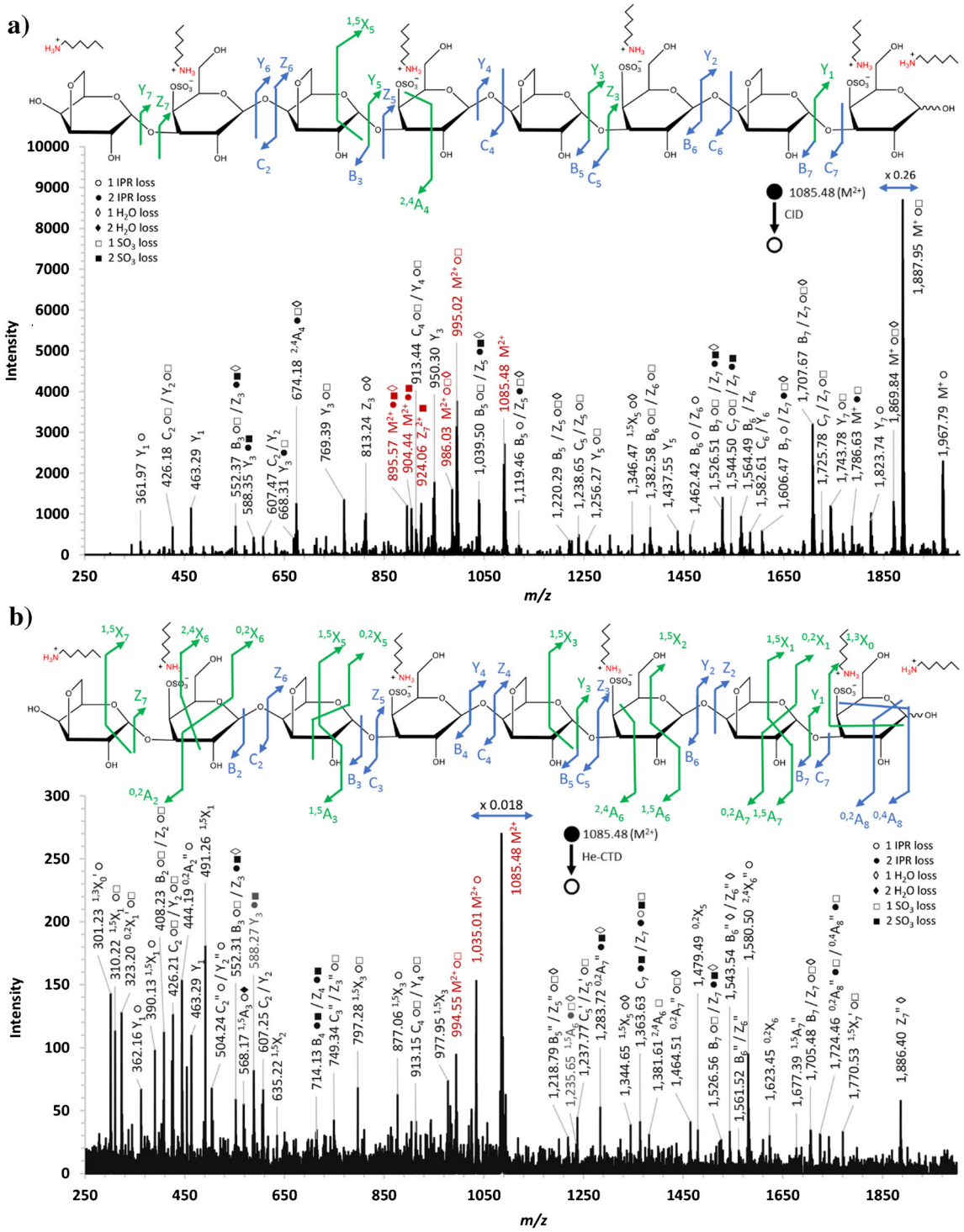

Fig. 4 IP-RP-UHPLC-MS/MS spectra of κ-carrageenan DP8 eluting at 3.7 min using **a)** LE-CID and **b)** He-CTD. The insets show the annotated product ions. Fragments with unambiguous assignments are annotated in green, ambiguous assignments are annotated in blue, and annotations in red are doubly charged. The notation M^+ in the labels refers to the precursor $[M + 6IPRH]^{2+}$ species, which was selected as the isolated precursor ion at *m/z* 1085.48

the doubly charged precursor ion at *m/z* 1085.48 was isolated and fragmented using both CID and He-CTD. Similar to κ-DP4, the LE-CID spectrum in Fig. 4a for κ-DP8 contains abundant B/Y and C/Z glycosidic fragments [22, 27, 71]. The LE-CID spectrum is populated with neutral losses of H_2O, IP reagent, and SO_3, which complicates the spectrum and provides redundant information. Compared to the LE-CID spectrum of κ-DP4, the doubly charged κ-DP8 produced

a larger number of unambiguous glycosidic cleavages and less abundant fragments corresponding to cross-ring cleavages. The unambiguous glycosidic pairs, Y_1/Y_3, Y_3/Y_5, and Y_5/Y_7, can be used to identify the repeating unit composition of κ-DP8 (DA-G4S) [17, 27]. Fragments corresponding to $^{2,4}A_n$ have been reported for CID of sodium adducted κ-DP6 [71], but the related fragments were not observed here using IPR adducts of κ-DP4 or κ-DP6. However, $^{2,4}A_n$ fragments were abundant in the CID spectrum of the κ-DP8 structure in the 2+ charge state bound with 6 IPR groups. The presence of the Y_5 and $^{2,4}A_4$ fragment pair in κ-DP8 helps to narrow down the sulfation position to 3rd and 4th position of the G4S unit. In the absence of prior knowledge about the structure, additional cross-ring cleavages such as $^{0,2}A_n$ and $^{0,2}X_{n-1}$ are needed to provide an accurate location of the 4-*O* sulfate group because of the isomeric nature of $^{2,4}A_4$ and $^{1,3}A_4$.

In contrast to the LE-CID spectrum of κ-DP8 in Fig. 4a, the He-CTD spectrum in Fig. 4b produced a series of abundant $^{1,5}X_n$, $^{0,2}X_n$, $^{1,5}A_n$, and $^{0,2}A_n$ cross-ring fragments, which is reminiscent of He-CTD of the same oligosaccharides studied in negative ion mode [17]. A similar series of cross-ring fragments have also been reported with XUV-PD with synchrotron radiation for κ-DP6 in the presence of heptyl ammonium as the IP agent [43]. Likewise, in ESM Fig. S1b, the He-CTD spectrum of κ-DP12 shows a series of unambiguous $^{1,5}X_n$ and $^{0,2}A_n$ fragments, which are not observed in the corresponding LE-CID spectrum (ESM Fig. S1a).

The series of unambiguous cross-ring cleavages in the He-CTD spectra provides evidence that He-CTD is equally effective with larger oligosaccharides, such as DP8 and DP12, as it is for smaller oligosaccharides. κ-DP12 is greater than 3 kDa in mass, and CTD fragmentation of the 2+ precursor generally preserved the six labile sulfate groups. In these experiments, reducing end labelling was not performed, which can lead to mis-assignments in peak annotation. However, labelling with heavy oxygen (^{18}O) has been used successfully in the past to help differentiate ions originating from the reducing and non-reducing termini [1, 32].

Figures 5, 6, and 7 show the fragments observed for κ-DP6, ι-DP6, and λ-DP6, respectively, using both LE-CID and He-CTD. ESM Fig. S3 shows the LE-CID and He-CTD product ion spectra for κ-DP6 from which the fragment ion maps in Fig. 5 were derived. Figure 5a shows that LE-CID was able to determine the monomeric composition of κ-DP6 through the generated glycosidic cleavages. The Y_5 fragment helped to distinguish the DA monomers at the non-reducing ends, whereas the Y_3/Y_5 fragment pair provided the repeating disaccharide unit composition (DA-G4S) of κ-DP6 [22, 27, 71].

In contrast to LE-CID, He-CTD provided a series of $^{1,5}X_n$ and $^{0,2}A_n$ cross-ring cleavages for κ-DP6, as shown in Fig. 5b. Again, the types of fragments formed in He-CTD are similar to those formed in XUV-PD [43] and negative mode CTD [17]. The $^{1,5}X_n$ and $^{0,2}A_n$ ions were also characteristic in the He-CTD spectra for κ-DP4, κ-DP8, and κ-DP12 in Figs. 3b and 4b and ESM Fig. S2b, respectively. The majority of the cross-ring fragmentation products can be seen throughout the structure, and many monosaccharide units have undergone multiple cross-ring cleavages, as described before [17]. Similar to LE-CID, repeating unit DA-G4S is identified by the glycosidic cleavage pairs Y_1 and Y_3. He-CTD also generated $^{2,4}A_n$ fragments with κ-carrageenans, which has previously been reported with ECD in the presence of divalent metal adducted κ-carrageenans [36]. Cross-ring cleavages, such as $^{2,4}A_n$ and $^{0,2}A_n$, can help locate the 4-*O* sulfation group in κ- and ι- carrageenans [17]. 4-*O* sulfation is also found in GAGs, including dermatan sulfate and chondroitin sulfate, which is difficult to locate with EDD and NETD because they tend to form less abundant $^{2,4}A_n$ or $^{2,4}X_n$ fragments [21, 35, 38]. With the He-CTD results and the prior knowledge about the glycosidic linkage position, the $^{2,4}A_4/Z_3$ fragments place the sulfate position at the 3rd or 4th position on the G4S unit [2]. Without the prior knowledge of the structure, additional cross-ring fragments, such as $^{0,2}A_n$, are needed to accurately locate the 4-*O* sulfation under these conditions.

ι-DP6 eluted at 5.9 min and contains the DA2S-G4S repeating disaccharide unit with a sulfate group on each monosaccharide unit. Figure 6 shows the fragment ion maps of ι-DP6 with LE-CID and He-CTD that were derived from the product ion spectra in ESM Figs. S4a and S4b. As expected, LE-CID generated a majority of glycosidic fragments, some prominent Y_n ions, and an extensive series of neutral losses of IPR, H_2O, and SO_3, which inundate the spectrum with redundant information in a similar fashion to LE-CID of κ-DP4 and κ-DP6. The repeating unit DA2S-G4S is identified with the Y_1/Y_3 and Y_3/Y_5 fragment pairs, but the lack of cross-ring fragments makes it difficult to localize the 2-*O* and 4-*O* sulfate modification on individual monomeric units. In contrast to LE-CID, He-CTD produced both glycosidic cleavages and a rich set of cross-ring cleavages, with many more fragments retaining the sulfate groups compared to LE-CID. Again, these results mirror the findings of the same structures in negative ion mode CTD [17].

The He-CTD fragment ion map of ι-DP6 shows prominent $^{1,5}X_n$ and $^{0,2}X_n$ product ions [17]. The $^{1,5}X_n$ fragments are abundant towards the reducing end, which is similar to the various κ-carrageenans, whereas $^{0,2}X_n$ fragments tend to be more abundant towards the non-reducing end [17]. This pattern is somewhat unique in ι-carrageenans relative to κ- and λ-carrageenans. The generation of $^{0,2}X_n$ fragments helps localize the 2-*O* sulfation group, which is more valuable for the ι-carrageenans compared to the κ-carrageenans. Even without prior knowledge of glycosidic linkage positions among the DA2S and G4S units, the unambiguous fragment pairs of

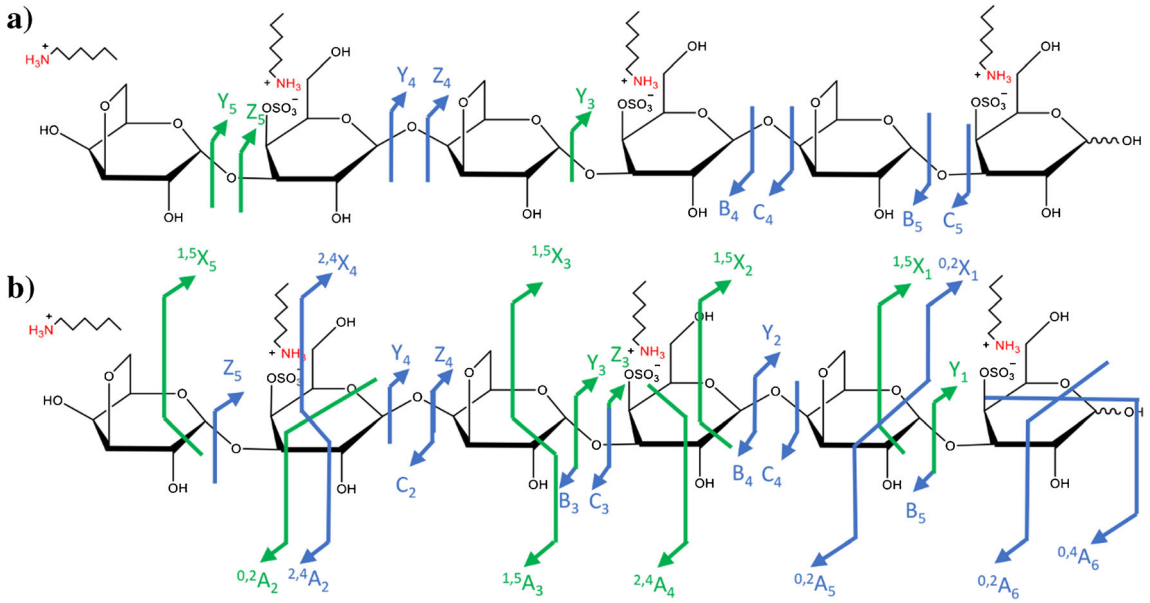

Fig. 5 Fragment ion maps for κ-DP6 at 2.6 min with **a)** LE-CID and **b)** He-CTD. Blue annotations are ambiguous because of alternative isobaric annotations and green annotations are unambiguous

$^{0,2}X_3/^{1,5}A_3$ can be used to localize the 2-*O* sulfation on the DA2S monomers. The absence of unambiguous glycosidic cleavages at the center of the molecule makes it difficult to identify the repeating unit of the structure.

Identification of the 2-linked modifications in monomer units is not only important for ι- and λ-carrageenans but is also important in the analysis of GAGs samples. For example, EDD and NETD are used as powerful tools in the analysis of GAGs because they are capable of producing $^{0,2}A_n$, $^{0,2}X_n$, and $^{1,5}X_n$ fragments and confirm the 2-*O* sulfation on glucuronic acid (GlcA) and 2-*N* sulfation on glucosamine [21, 35]. In the presence of an anhydro bridge in the ring structure, only $^{1,5}X_n$, $^{0,2}X_n$, and $^{0,2}A_n$ fragments were produced, which limits the information that can be harvested about the linkage positions among the DA2S and G4S units [17, 43]. However, the presence of $^{0,2}A_2$, $^{0,2}X_3$, and $^{1,5}A_3$ product ions helps to obtain the linkage details of the DA2S unit. The previous comparison of He-CTD and EDD of GAGs in negative ion mode [21] and the demonstration that He-CTD is highly effective for the 2-*O* sulfated carrageenans in positive mode both indicate that He-

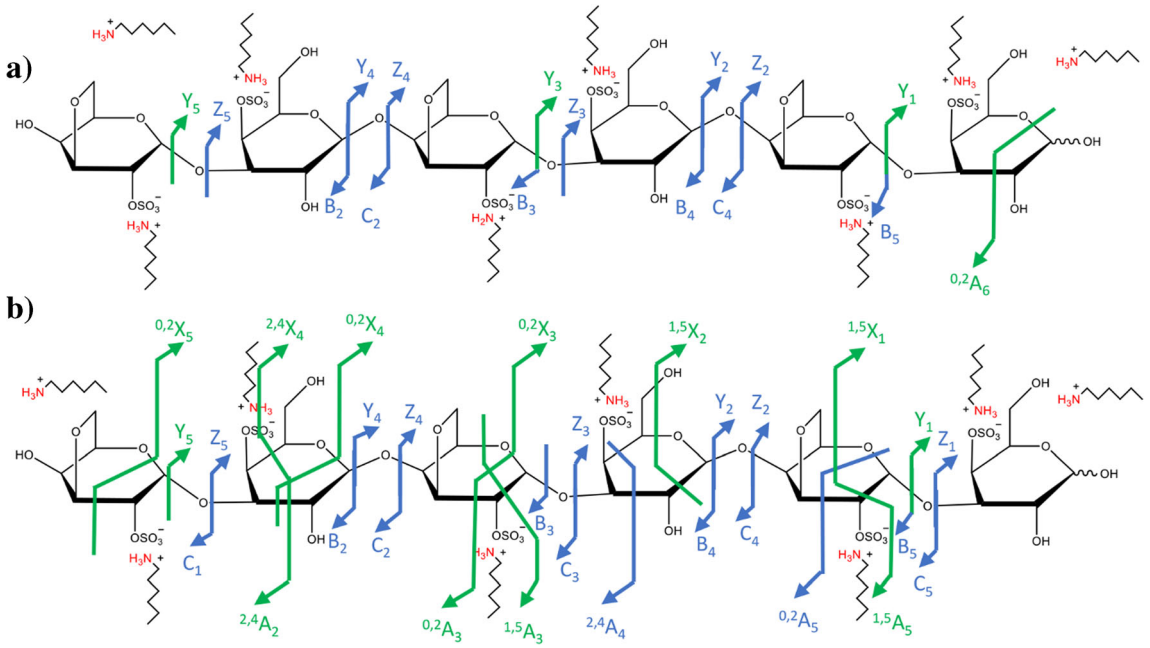

Fig. 6 Fragment ion maps for ι-DP6 at 5.9 min with **a)** LE-CID and **b)** He-CTD. Blue annotations are ambiguous because of alternative isobaric annotations and green annotations are unambiguous

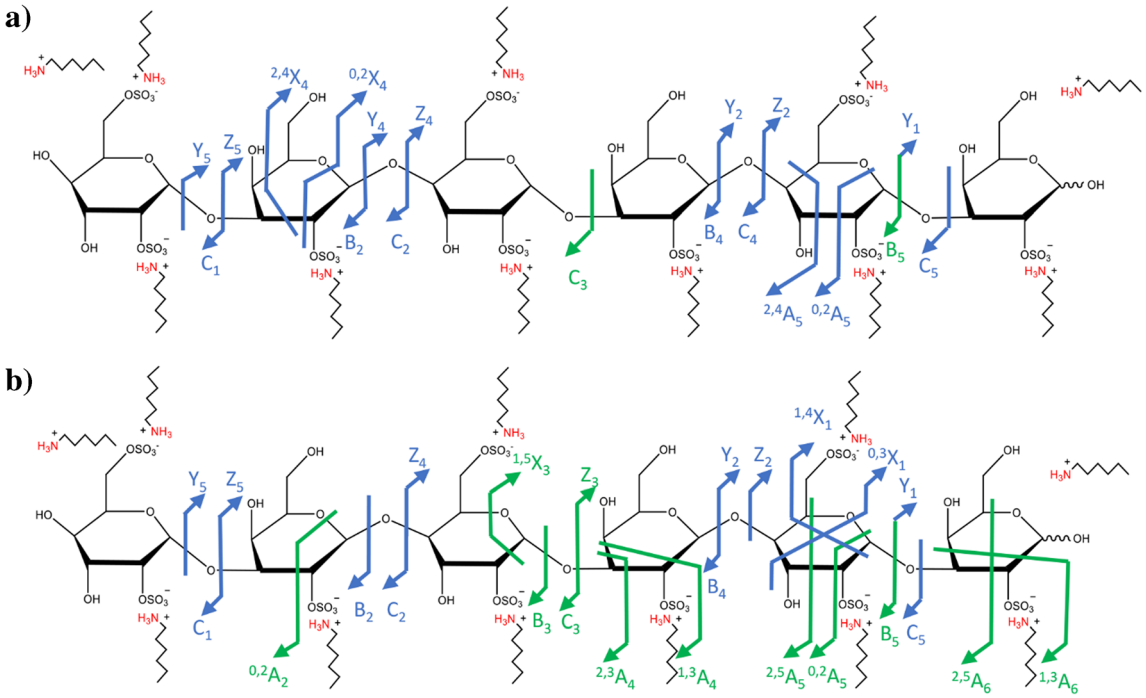

Fig. 7 Fragment ion maps for λ-DP6 at 7.9 min with **a)** LE-CID and **b)** He-CTD. Blue annotations are ambiguous because of alternative isobaric annotations and green annotations are unambiguous

CTD of GAGs in positive mode ought to be compatible with HPLC-based separations of complex mixtures of GAGs in the future.

Compared to both κ- and ι-carrageenans, λ-carrageenans have more sulfate modifications throughout their backbone, with three sulfate groups on each pair of repeating disaccharide unit (D2S,6S-G2S), as shown in Fig. 7. The 2+ precursor ion at *m/z* 1412.64 contains 9 negatively charged sulfate groups and 11 non-covalent, positively charged ion-pair-reagent ions. ESM Fig. S5a shows that LE-CID was able to produce mainly the glycosidic cleavages throughout the precursor and fewer cross-ring cleavages than He-CTD, but the absence of heavy oxygen labelling means that only the C_3 and B_5 fragments are unambiguous fragments. The repeating unit D2S,6S-G2S is identified with the C_3/B_5 fragment pair. Similar to LE-CID of the κ- and ι-carrageenans, LE-CID of λ-DP6 did not provide any significant unambiguous cross-ring cleavages, which therefore limits the information regarding sulfate group positions within each monomer.

However, despite the presence of 11 non-covalently bound adducts, the He-CTD produced both glycosidic and high-energy cross-ring fragments, with a majority of the cross-ring fragments localized towards the reducing end and a majority of the unambiguous glycosidic fragments localized on the glycosidic bond between the D2S,6S and G2S units at the center (ESM Fig. S5b). D2S,6S monomers in the non-reducing end of the structure do not show any possible cross-ring fragments, and only the D2S,6S monomer at the reducing end shows multiple cross-ring cleavages, including unambiguous $^{0,2}A_5$ and $^{2,5}A_5$ and ambiguous $^{1,4}X_1$ and $^{0,3}X_1$. The D2S,6S-G2S repeating unit is identified by the glycosidic fragment pairs B_3/B_5. The 2-linked sulfate group on the G2S monomer in the reducing end of the structure can be localized with the aid of the $^{1,3}A_6/^{2,5}A_6$ fragment pair, which is not possible with the LE-CID spectrum. He-CTD therefore provides significantly more structural information than LE-CID, but the limited number of cross-ring fragments and their localization towards the reducing end limits the amount of information that is available to locate the 6-*O* sulfation on the D2S,6S monomer in λ-DP6.

A visual comparison of different fragment ion types including glycosidic fragment, glycosidic fragment -SO_3 loss, cross-ring fragment, and cross-ring fragment -SO_3 loss for κ-, ι-, and λ-carrageenans (DP6) is shown in Fig. 8. The generated donut plots display percentages of the summed ion intensity of fragment ion types produced with LE-CID and He-CTD for the three carrageenan categories. The plots show that LE-CID is less likely to produce abundant cross-ring fragments compared to He-CTD. Among the glycosidic fragments generated with LE-CID, λ-carrageenan shows a higher percentage of sulfate groups retained with glycosidic fragments at 53%. He-CTD of κ-DP6 shows the highest percentage of cross-ring fragments at 48.5% and has the lowest percentage of sulfate losses for both glycosidic and cross-ring fragment types at 37.8%. In

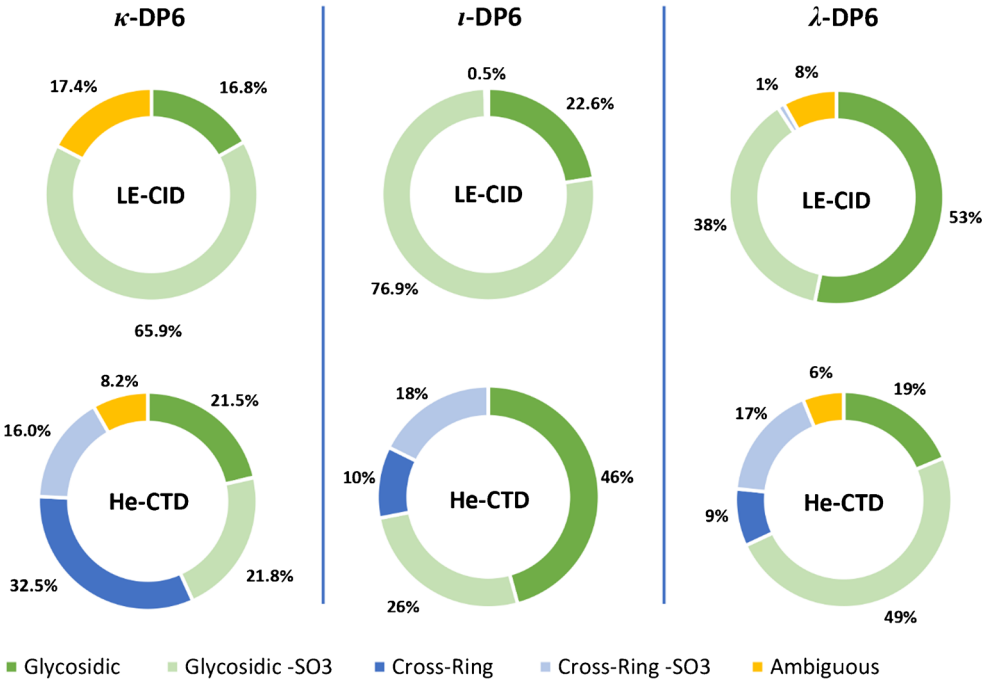

Fig. 8 Charts to show the relative distribution of fragment ion abundances for κ-DP6, ι-DP6, and λ-DP6 carrageenan. In general, cross-ring cleavages in dark blue are considered desirable

future He-CTD studies, different charge states of carrageenans should be investigated to identify the optimum charge state for each subclass to maximize the preservation of labile sulfate groups [73, 74].

Conclusion

In this study, we have demonstrated the applicability of online He-CTD for the analysis of a complex sulfated oligosaccharide mixture, which contains kappa (κ), iota (ι), and lambda (λ) carrageenans with different degrees of polymerization (DP) (between DP4-12), anhydro bridges, different degrees of sulfation ranging from one to three per dimer, and different positioning of the sulfate groups along the backbone. Our results demonstrate that He-CTD is compatible with the timescales and sample loads required for UHPLC and provides spectra with adequate S/N ratios to enable extensive structural information while achieving comparable performances with EDD, NETD, and XUV-PD. In contrast to LE-CID, more of the He-CTD product ions retain the labile sulfate groups. Even in the absence of ^{18}O-labelling, He-CTD provided a series of informative and unambiguous fragments corresponding to high-energy, radical-induced cross-ring cleavages from both the reducing end and non-reducing ends, such as $^{1,5}X_n$, $^{0,2}X_n$, and $^{0,2}A_n$ product ions. With the exception of the 1,5-cleavages, the A_n and X_n ions provide useful linkage information that is not typically possible using LE-CID. Similar to LE-CID, He-CTD also generates glycosidic bond cleavages, which provides additional information about the dimeric repeating sequence of each carrageenan oligosaccharide. This work highlights the efficient use of He-CTD activation directly coupled with a separation technique for the characterization of complex mixtures and opens up possible applications in the food, pharmaceutical or medical industries.

Supplementary Information The online version contains supplementary material available at https://doi.org/10.1007/s00216-021-03396-3.

Acknowledgements The opinions, findings, and conclusions or recommendations expressed in this publication are those of the author(s) and do not necessarily reflect the views of NSF or NIH. The authors thank Dr. C. Hervé and M. Jam (CNRS-UPMC UMR 8227, Station Biologique, Roscoff, France) for providing the oligosaccharides.

Funding This work was supported by the National Science Foundation (NSF) (CHE-1710376) and the National Institute of Health (NIH) (1R01GM114494-01).

Declarations

Conflict of interest The authors declare no competing interests.

References

1. Ropartz D, Lemoine J, Giuliani A, Bittebière Y, Enjalbert Q, Antoine R, et al. Deciphering the structure of isomeric oligosaccharides in a complex mixture by tandem mass spectrometry: photon activation with vacuum ultra-violet brings unique information and

enables definitive structure assignment. Anal Chim Acta. 2014;807:84–95. https://doi.org/10.1016/j.aca.2013.11.018.
2. Antonopoulos A, Favetta P, Helbert W, Lafosse M. Isolation of κ-carrageenan oligosaccharides using ion-pair liquid chromatography - characterisation by electrospray ionisation mass spectrometry in positive-ion mode. Carbohydr Res. 2004;339:1301–9. https://doi.org/10.1016/j.carres.2004.03.002.
3. Campo VL, Kawano DF, Braz D, Carvalho I. Carrageenans : biological properties , chemical modifications and structural analysis – a review. Carbohydr Polym 2009;77:167–180. https://doi.org/10.1016/j.carbpol.2009.01.020.
4. Campbell R, Hotchkiss S. Carrageenan industry market overview. In: Hurtado AQ, Critchley AT, Neish IC, editors. Trop. Seaweed Farming Trends, Probl. Oppor., Cham: Springer International Publishing; 2017, p. 193–205. https://doi.org/10.1007/978-3-319-63498-2_13.
5. Li L, Ni R, Shao Y, Mao S. Carrageenan and its applications in drug delivery. Carbohydr Polym. 2014;103:1–11. https://doi.org/10.1016/j.carbpol.2013.12.008.
6. Yermak IM, Barabanova AO, Aminin DL, Davydova VN, Sokolova EV, Solov'Eva TF, et al. Effects of structural peculiarities of carrageenans on their immunomodulatory and anticoagulant activities. Carbohydr Polym. 2012;87:713–20. https://doi.org/10.1016/j.carbpol.2011.08.053.
7. Panlasigui LN, Baello OQ, Dimatangal JM, Dumelod BD. Blood cholesterol and lipid-lowering effects of carrageenan on human volunteers. Asia Pac J Clin Nutr. 2003;12:209–14.
8. Cáceres PJ, Carlucci MJ, Damonte EB, Matsuhiro B, Zúñiga EA. Carrageenans from chilean samples of Stenogramme interrupta (Phyllophoraceae): structural analysis and biological activity. Phytochemistry. 2000;53:81–6. https://doi.org/10.1016/S0031-9422(99)00461-6.
9. Sun Y, Liu Y, Jiang K, Wang C, Wang Z, Huang L. Electrospray ionization mass spectrometric analysis of κ-carrageenan oligosaccharides obtained by degradation with κ-carrageenase from Pedobacter hainanensis. J Agric Food Chem. 2014;62:2398–405. https://doi.org/10.1021/jf500429r.
10. Girond S, Crance JM, Van Cuyck-Gandre H, Renaudet J, Deloince R. Antiviral activity of carrageenan on hepatitis A virus replication in cell culture. Res Virol. 1991;142:261–70. https://doi.org/10.1016/0923-2516(91)90011-Q.
11. Talarico LB, Zibetti RGM, Faria PCS, Scolaro LA, Duarte MER, Noseda MD, et al. Anti-herpes simplex virus activity of sulfated galactans from the red seaweeds Gymnogongrus griffithsiae and Cryptonemia crenulata. Int J Biol Macromol. 2004;34:63–71. https://doi.org/10.1016/j.ijbiomac.2004.03.002.
12. Ana P, Nathalie B, Gilles B, Daniel R, Tomás M, Yolanda F. Anti-herpes simplex virus (HSV-1) activity and antioxidant capacity of carrageenan-rich enzymatic extracts from Solieria filiformis (Gigartinales, Rhodophyta). Int J Biol Macromol. 2021;168:322–30. https://doi.org/10.1016/j.ijbiomac.2020.12.064.
13. Wang W, Zhang P, Yu GL, Li CX, Hao C, Qi X, et al. Preparation and anti-influenza A virus activity of κ-carrageenan oligosaccharide and its sulphated derivatives. Food Chem. 2012;133:880–8. https://doi.org/10.1016/j.foodchem.2012.01.108.
14. Jang Y, Shin H, Lee MK, Kwon OS, Shin JS, Kim Y il, et al. Antiviral activity of lambda-carrageenan against influenza viruses and severe acute respiratory syndrome coronavirus 2. Sci Rep. 2021;11:1–12. https://doi.org/10.1038/s41598-020-80896-9.
15. Talarico LB, Damonte EB. Interference in dengue virus adsorption and uncoating by carrageenans. Virology. 2007;363:473–85. https://doi.org/10.1016/j.virol.2007.01.043.
16. Piccini LE, Carro AC, Quintana VM, Damonte EB. Antibody-independent and dependent infection of human myeloid cells with dengue virus is inhibited by carrageenan. Virus Res. 2020;290:198150. https://doi.org/10.1016/j.virusres.2020.198150.
17. Ropartz D, Li P, Jackson GP, Rogniaux H. Negative polarity helium charge transfer dissociation tandem mass spectrometry: radical-initiated fragmentation of complex polysulfated anions. Anal Chem. 2017;89(7):3824–8. https://doi.org/10.1021/acs.analchem.7b00473.
18. Antonopoulos A, Favetta P, Helbert W, Lafosse M. On-line liquid chromatography-electrospray ionisation mass spectrometry for κ-carrageenan oligosaccharides with a porous graphitic carbon column. J Chromatogr A. 2007;1147:37–41. https://doi.org/10.1016/j.chroma.2007.02.023.
19. Ackloo S, Terlouw JK, Ruttink PJA, Burgers PC. Analysis of carrageenans by matrix-assisted laser desorption/ionization and electrospray ionization mass spectrometry. I kappa-Carrageenans Rapid Commun Mass Spectrom. 2001;15:1152–9. https://doi.org/10.1002/rcm.351.
20. Zaia J. On-line separations combined with MS for analysis of glycosaminoglycans. Mass Spectrom Rev. 2009;28:254–72. https://doi.org/10.1002/mas.20200.
21. Pepi LE, Sasiene ZJ, Mendis PM, Jackson GP, Amster IJ. Structural characterization of sulfated glycosaminoglycans using charge-transfer dissociation. J Am Soc Mass Spectrom. 2020. https://doi.org/10.1021/jasms.0c00252.
22. Aguilan JT, Dayrit FM, Zhang J, Ninonuevo MR, Lebrilla CB. Structural analysis of k-carrageenan sulfated oligosaccharides by positive mode Nano-ESI-FTICR-MS and MS/MS by SORI-CID. J Am Soc Mass Spectrom. 2006;17:96–103. https://doi.org/10.1016/j.jasms.2005.09.009.
23. Guibet M, Kervarec N, Génicot S, Chevolot Y, Helbert W. Complete assignment of 1H and 13C NMR spectra of Gigartina skottsbergii λ-carrageenan using carrabiose oligosaccharides prepared by enzymatic hydrolysis. Carbohydr Res. 2006;341:1859–69. https://doi.org/10.1016/j.carres.2006.04.018.
24. Chauhan PS, Saxena A. Bacterial carrageenases: an overview of production and biotechnological applications. 3. Biotech. 2016;6:146. https://doi.org/10.1007/s13205-016-0461-3.
25. Yu G, Guan H, Ioanoviciu AS, Sikkander SA, Thanawiroon C, Tobacman JK, et al. Structural studies on κ-carrageenan derived oligosaccharides. Carbohydr Res. 2002;337:433–40. https://doi.org/10.1016/S0008-6215(02)00009-5.
26. Antonopoulos A, Herbreteau B, Lafosse M, Helbert W. Comparative analysis of enzymatically digested κ-carrageenans, using liquid chromatography on ion-exchange and porous graphitic carbon columns coupled to an evaporative light scattering detector. J Chromatogr A. 2004;1023:231–8. https://doi.org/10.1016/j.chroma.2003.10.011.
27. Ekeberg D, Knutsen SH, Sletmoen M. Negative-ion ESI–MS as a tool for analysing structural heterogeneity in kappa-carrageenan oligosaccharides. Carbohydr Res. 2001;334:49–59.
28. Han L, Costello CE. Mass spectrometry of glycans. Biochem. 2013;78:710–20. https://doi.org/10.1134/s0006297913070031.
29. Wuhrer M, Deelder AM, van der Burgt YEM. Mass spectrometric glycan rearrangements. Mass Spectrom Rev. 2011;30:664–80. https://doi.org/10.1002/mas.20337.
30. Zaia J, Miller MJC, Seymour JL, Costello CE. The role of mobile protons in negative ion CID of oligosaccharides. J Am Soc Mass Spectrom. 2007;18:952–60. https://doi.org/10.1016/j.jasms.2007.01.016.
31. Zaia J, McClellan JE, Costello CE. Tandem mass spectrometric determination of the 4S/6S sulfation sequence in chondroitin sulfate oligosaccharides. Anal Chem. 2001;73:6030–9. https://doi.org/10.1021/ac015577t.
32. Ropartz D, Li P, Fanuel M, Giuliani A, Rogniaux H, Jackson GP. Charge transfer dissociation of complex oligosaccharides: comparison with collision-induced dissociation and extreme ultraviolet dissociative photoionization. J Am Soc Mass Spectrom. 2016;27:1614–9. https://doi.org/10.1007/s13361-016-1453-6.

33. Wolff JJ, Amster IJ, Chi L, Linhardt RJ. Electron detachment dissociation of glycosaminoglycan tetrasaccharides. J Am Soc Mass Spectrom. 2007;18:234–44. https://doi.org/10.1016/j.jasms.2006.09.020.
34. Wolff JJ, Chi L, Linhardt RJ, Amster IJ. Distinguishing glucuronic from iduronic acid in glycosaminoglycan tetrasaccharides by using electron detachment dissociation. Anal Chem. 2007;79:2015–22. https://doi.org/10.1021/ac061636x.
35. Leach lll FE, Riley NM, Westphall MS, Coon JJ, Amster IJ. Negative electron transfer dissociation sequencing of increasingly sulfated glycosaminoglycan oligosaccharides on an Orbitrap mass spectrometer. J Am Soc Mass Spectrom 2017;28:1844–1854. https://doi.org/10.1007/s13361-017-1709-9.
36. Liu H, Hakansson K. Electron capture dissociation of divalent metal-adducted sulfated oligosaccharides. Int J Mass Spectrom. 2011;305:170–7. https://doi.org/10.1016/j.ijms.2010.10.030.
37. Wolff JJ, Laremore TN, Aslam H, Linhardt RJ, Amster IJ. Electron-induced dissociation of glycosaminoglycan tetrasaccharides. J Am Soc Mass Spectrom. 2008;19:1449–58. https://doi.org/10.1016/j.jasms.2008.06.024.
38. Leach lll FE, Ly M, Laremore TN, Wolff JJ, Perlow J, Linhardt RJ, et al. Hexuronic acid stereochemistry determination in chondroitin sulfate glycosaminoglycan oligosaccharides by electron detachment dissociation. J Am Soc Mass Spectrom. 2012;23:1488–97. https://doi.org/10.1007/s13361-012-0428-5.
39. Herron WJ, Goeringer DE, McLuckey SA. Gas-phase electron transfer reactions from multiply-charged anions to rare gas cations. J Am Chem Soc. 1995;117:11555–62. https://doi.org/10.1021/ja00151a021.
40. Klein DR, Leach lll FE, Amster IJ, Brodbelt JS. Structural characterization of glycosaminoglycan carbohydrates using ultraviolet photodissociation. Anal Chem 2019;91:6019–6026. https://doi.org/10.1021/acs.analchem.9b00521.
41. Fort KL, Cramer CN, Voinov VG, Vasil YV, Lopez NI, Beckman JS, et al. Exploring ECD on a benchtop Q Exactive Orbitrap mass spectrometer. J Proteome Res. 2018;17:926–33. https://doi.org/10.1021/acs.jproteome.7b00622.
42. Ropartz D, Giuliani A, Hervé C, Geairon A, Jam M, Czjzek M, et al. High-energy photon activation tandem mass spectrometry provides unprecedented insights into the structure of highly sulfated oligosaccharides extracted from macroalgal cell walls. Anal Chem. 2015;87:1042–9. https://doi.org/10.1021/ac5036007.
43. Ropartz D, Giuliani A, Fanuel M, Hervé C, Czjzek M, Rogniaux H. Online coupling of high-resolution chromatography with extreme UV photon activation tandem mass spectrometry: application to the structural investigation of complex glycans by dissociative photoionization. Anal Chim Acta. 2016;933:1–9. https://doi.org/10.1016/j.aca.2016.05.036.
44. Wilson JJ, Brodbelt JS. Ultraviolet photodissociation at 355 nm of fluorescently labeled oligosaccharides. Anal Chem. 2008;80:5186–96. https://doi.org/10.1021/ac800315k.
45. Reilly JP. Ultraviolet photofragmentation of biomolecular ions. Mass Spectrom Rev. 2009;28:425–47. https://doi.org/10.1002/mas.20214.
46. Devakumar A, Mechref Y, Kang P, Novotny MV, Reilly JP. Laser-induced photofragmentation of neutral and acidic glycans inside an ion-trap mass spectrometer. Rapid Commun Mass Spectrom. 2007;21:1452–60. https://doi.org/10.1002/rcm.2981.
47. Devakumar A, Mechref Y, Kang P, Novotny MV, Reilly JP. Identification of isomeric N-glycan structures by mass spectrometry with 157 nm laser-induced photofragmentation. J Am Soc Mass Spectrom. 2008;19:1027–40. https://doi.org/10.1016/j.jasms.2008.03.005.
48. Devakumar A, Thompson MS, Reilly JP. Fragmentation of oligosaccharide ions with 157 nm vacuum ultraviolet light. Rapid Commun Mass Spectrom. 2005;19:2313–20. https://doi.org/10.1002/rcm.2058.
49. Murtada R, Fabijanczuk K, Gaspar K, Dong X, Alzarieni KZ, Calix K, et al. Free-radical-mediated glycan isomer differentiation. Anal Chem. 2020;92:13794–802. https://doi.org/10.1021/acs.analchem.0c02213.
50. Desai N, Thomas DA, Lee J, Gao J, Beauchamp JL. Eradicating mass spectrometric glycan rearrangement by utilizing free radicals. Chem Sci. 2016;7:5390–7. https://doi.org/10.1039/c6sc01371f.
51. Hoffmann WD, Jackson GP. Charge transfer dissociation (CTD) mass spectrometry of peptide cations using kiloelectronvolt helium cations. J Am Soc Mass Spectrom. 2014;25:1939–43. https://doi.org/10.1007/s13361-014-0989-6.
52. Sasiene ZJ, Mendis PM, Jackson GP. Quantitative assessment of six different reagent gases for charge transfer dissociation (CTD) of biological ions. Int J Mass Spectrom. 2021;462:116532. https://doi.org/10.1016/j.ijms.2021.116532.
53. Li P, Kreft I, Jackson GP. Top-down charge transfer dissociation (CTD) of gas-phase insulin: evidence of a one-step, two-electron oxidation mechanism. J Am Soc Mass Spectrom. 2018;29:284–96. https://doi.org/10.1007/s13361-017-1700-5.
54. Li P, Jackson GP. Charge transfer dissociation (CTD) of phosphocholines: gas-phase ion/ion reactions between helium cations and phospholipid cations. J Mass Spectrom. 2017;52:271–82. https://doi.org/10.1002/jms.3926.
55. Bari S, Hoekstra R, Schlathölter T. Peptide fragmentation by keV ion-induced dissociation. Phys Chem Chem Phys. 2010;12:3317–632. https://doi.org/10.1039/b924145k.
56. Chingin K, Makarov A, Denisov E, Rebrov O, Zubarev RA. Fragmentation of positively-charged biological ions activated with a beam of high-energy cations. Anal Chem. 2014;86:372–9. https://doi.org/10.1021/ac403193k.
57. Bari S, Hoekstra R, Schlathölter T. Fast side-chain losses in keV ion-induced dissociation of protonated peptides. Int J Mass Spectrom. 2011;299:64–70. https://doi.org/10.1016/j.ijms.2010.09.019.
58. Buck-Wiese H, Fanuel M, Liebeke M, Le Mai HK, Pardo-Vargas A, Seeberger PH, et al. Discrimination of β-1,4- and β-1,3-linkages in native oligosaccharides via charge transfer dissociation mass spectrometry. J Am Soc Mass Spectrom. 2020;31:1249–59. https://doi.org/10.1021/jasms.0c00087.
59. Doneanu CE, Chen W, Gebler JC. Analysis of oligosaccharides derived from heparin by ion-pair reversed-phase chromatography/mass spectrometry. Anal Chem. 2009;81:3485–99. https://doi.org/10.1021/ac802770r.
60. Thanawiroon C, Linhardt RJ. Separation of a complex mixture of heparin-derived oligosaccharides using reversed-phase high-performance liquid chromatography. J Chromatogr A. 2003;1014:215–23. https://doi.org/10.1016/S0021-9673(03)00779-9.
61. Thanawiroon C, Rice KG, Toida T, Linhardt RJ. Liquid chromatography/mass spectrometry sequencing approach for highly sulfated heparin-derived oligosaccharides. J Biol Chem. 2004;279:2608–15. https://doi.org/10.1074/jbc.M304772200.
62. Liu H, Joshi A, Chopra P, Liu L, Boons GJ, Sharp JS. Salt-free fractionation of complex isomeric mixtures of glycosaminoglycan oligosaccharides compatible with ESI-MS and microarray analysis. Sci Rep. 2019;9:1–13. https://doi.org/10.1038/s41598-019-53070-z.

63. Hitchcock AM, Costello CE, Zaia J. Glycoform quantification of chondroitin/dermatan sulfate using a liquid chromatography-tandem mass spectrometry platform. Biochemistry. 2006;45:2350–61. https://doi.org/10.1021/bi052100t.
64. Naimy H, Leymarie N, Bowman MJ, Zaia J. Characterization of heparin oligosaccharides binding specifically to antithrombin III using mass spectrometry. Biochemistry. 2008;47:3155–61. https://doi.org/10.1021/bi702043e.
65. Wu J, Wei J, Chopra P, Boons GJ, Lin C, Zaia J. Sequencing heparan sulfate using HILIC LC-NETD-MS/MS. Anal Chem. 2019;91:11738–46. https://doi.org/10.1021/acs.analchem.9b02313.
66. Pabst M, Altmann F. Influence of electrosorption, solvent, temperature, and ion polarity on the performance of LC-ESI-MS using graphitic carbon for acidic oligosaccharides. Anal Chem. 2008;80:7534–42. https://doi.org/10.1021/ac801024r.
67. Mendis PM, Sasiene ZJ, Ropartz D, Rogniaux H, Jackson GP. Structural characterization of isomeric oligogalacturonan mixtures using ultrahigh-performance liquid chromatography-charge transfer dissociation mass spectrometry. Anal Chem. 2021;93:2838–47. https://doi.org/10.1021/acs.analchem.0c04142.
68. Kuberan B, Lech M, Zhang L, Wu ZL, Beeler DL, Rosenberg RD. Analysis of heparan sulfate oligosaccharides with ion pair-reverse phase capillary high performance liquid chromatography-microelectrospray ionization time-of-flight mass spectrometry. J Am Chem Soc. 2002;124:8707–18. https://doi.org/10.1021/ja0178867.
69. Fenner AM, Kerns RJ. Synthesis, separation, and characterization of amphiphilic sulfated oligosaccharides enabled by reversed-phase ion pairing LC and LC-MS methods. Carbohydr Res. 2011;346:2792–800. https://doi.org/10.1016/j.carres.2011.09.020.
70. Cook SL, Collin OL, Jackson GP. Metastable atom-activated dissociation mass spectrometry: Leucine/isoleucine differentiation and ring cleavage of proline residues. J Mass Spectrom. 2009;44:1211–23. https://doi.org/10.1002/jms.1598.
71. Gonçlves AG, Ducatti DRB, Grindley TB, Duarte MER, Nosedab MD. ESI-MS differential fragmentation of positional isomers of sulfated oligosaccharides derived from carrageenans and agarans. J Am Soc Mass Spectrom. 2010;21:1404–16. https://doi.org/10.1016/j.jasms.2010.03.045.
72. Domon B, Costello CE. A systematic nomenclature for carbohydrate fragmentations in FAB-MS/MS spectra of glycoconjugates. Glycoconj J. 1988;5:397–409. https://doi.org/10.1007/BF01049915.
73. Huang Y, Yu X, Mao Y, Costello CE, Zaia J, Lin C. De novo sequencing of heparan sulfate oligosaccharides by electron-activated dissociations. Anal Chem. 2013;85:11979–86. https://doi.org/10.1021/ac402931j.
74. Hu H, Huang Y, Mao Y, Yu X, Xu Y, Liu J, et al. A computational framework for heparan sulfate sequencing using high-resolution tandem mass spectra. Mol Cell Proteomics. 2014;13:2490–502. https://doi.org/10.1074/mcp.M114.039560.

Praneeth M. Mendis is a Ph.D. candidate at the C. Eugene Bennett Department of Chemistry in West Virginia University, Morgantown, WV, USA. His research focuses on online UHPLC coupled with charge transfer dissociation mass spectrometry (CTD-MS) of complex mixtures of oligosaccharides under the supervision of Dr. Glen P. Jackson.

Zachary J. Sasiene recently completed his Ph.D. with the dissertation title "Fundamentals and Applications of Charge Transfer Dissociation Mass Spectrometry" under the supervision of Dr. Glen P. Jackson at West Virginia University. His research interests include tandem mass spectrometry, ion trap mass spectrometry, and instrumentation modification. He has recently accepted a postdoctoral appointment at Los Alamos National Laboratory.

David Ropartz is the Mass Spectrometry Laboratory Manager of the UR BIA Biopolymers, Structural Biology Research Group at INRAE, France. His research focuses on the development of mass spectrometry tools for the characterization of polysaccharide structures, including alternative activation methods in MS/MS, ion-photon and ion-ion interactions, and improved separation and resolution of oligosaccharide isomers. He also employs high resolution in ion mobility spectrometry–mass spectrometry and mass spectrometry imaging for the study of the distribution of wall polysaccharides in plant systems.

Helene Rogniaux is a graduate scientist at INRAE, the French National Research Institute for Agriculture, Food and Environment in Nantes, France. Her research focuses on mass spectrometry for the structural characterization of bioresources and bioproducts, with particular expertise in structural glycosciences. Her latest results comprise the use of high-energy MS/MS fragmentation methods as well as of ion mobility for the determination of carbohydrate structures. She is also developing research in mass spectrometry imaging of polysaccharides in plant tissues.

Glen P. Jackson is the Ming Hsieh Distinguished Professor of Forensic and Investigative Science at West Virginia University. He also holds a joint appointment in the C. Eugene Bennett Department of Chemistry. He has published more than 80 articles related to mass spectrometric instrumentation development and forensic and biological applications. Since 2016, he has served as the co-founding co-Editor-in-Chief of the Elsevier journal *Forensic Chemistry*. He is also a member of the international advisory board for *Analytical and Bioanalytical Chemistry*.